Parallel Transport of BSA by Surface and Pore Diffusion in Strongly Basic Chitosan

Hiroyuki Yoshida, Motonobu Yoshikawa, and Takeshi Kataoka
Dept. of Chemical Engineering, University of Osaka Prefecture, Sakai 593, Japan

The parallel transport of a protein by surface and pore diffusion within a highly porous ion exchanger is studied by measuring equilibria and uptake curves for adsorption of bovine serum albumin (BSA) on two different strongly basic chitosan ion exchangers (hard gels): Ch-2503 and Ch-2507 at pH 6.9 and 298 K. Experimental equilibrium isotherms are correlated by the Langmuir equation. Intraparticle effective diffusivities of BSA (D_{eff}) are determined from the homogeneous Fickian diffusion model, increasing with the bulk phase concentration increase of BSA (C_0). It suggests the existence of parallel diffusion. The surface diffusivity D_S for the parallel diffusion model is determined from the D_{eff}, and $D_S = 0.47 \times 10^{-13}$ $m^2 \cdot s^{-1}$ (Ch-2507) and 2.4×10^{-13} $m^2 \cdot s^{-1}$ (Ch-2503) were obtained. Pore diffusivities based on the pore diffusion control (D'_P) are obtained by matching the shrinking core model with the experimental uptake curves. D'_P decreases with increasing C_0. Since D'_P in Ch-2507 is constant when $C_0 \geq 1$ $kg \cdot m^{-3}$, the constant value 2.7×10^{-11} $m^2 \cdot s^{-1}$ is taken as the accurate pore diffusivity (D_P). As D'_P in Ch-2503 does not approach a constant value, $D_P = 1.0 \times 10^{-11}$ $m^2 \cdot s^{-1}$ is determined by matching the parallel diffusion model with the uptake data, and the model calculated using experimental values of D_S and D_P agrees reasonably well with the uptake data for Ch-2507 and Ch-2503. This theoretical approach may be applied not only for intraparticle diffusion of proteins but any adsorbates in porous materials.

Introduction

The chromatographic separation of proteins is important not only for analyzing proteins but also for separating them in large-scale industries, such as the food and drug industry. A number of ion exchangers for separating proteins have been developed. In order to apply these ion-exchangers to large-scale chromatographic separation, it is necessary to investigate the equilibria, kinetics, and dynamics in detail.

The equilibrium isotherms for adsorption of bovine serum albumin (BSA) on DEAE-dextran (Yamamoto et al., 1983; Tsou and Graham, 1985) and on QAE-dextran (Yoshida et al., 1993) have been reported. Since these dextran ion exchangers are soft and compressed in a column, the bed shows extremely large pressure drop even when the flow rate is very slow (Pharmacia LKB Biotechnology, 1990). Therefore, it is difficult to use them for large-scale chromatographic separation. Recently, hard ion exchangers such as DEAE Sepharose Fast Flow (Pharmacia Fine Chemicals) and highly porous chitosan beads (Fuji Spinning Co.) have been developed to overcome the problem. As the pressure drops in their bed are small even in high flow rate, a high-pressure pump is not necessary (Yoshida et al., 1994). The equilibria for adsorption of BSA on the hard ion exchangers, weakly basic chitosan (Yoshida et al., 1989), DEAE Sepharose Fast Flow (James and Do, 1991; Yoshida et al., 1994), and strongly basic chitosan (Yoshida et al., 1994) have been investigated.

There have been several recent investigations for the intraparticle diffusion of proteins: a linear driving force model, that of an ion exchanger (Graham and Fook, 1982; Tsou and Graham, 1985); a homogeneous Fickian diffusion model, that of affinity separation (Arnold et al., 1985a,b); a pore diffusion model, that of affinity chromatography (Arve and Liapis, 1987, 1988; Liapis, 1990; McCoy and Liapis, 1991); displacement chromatography (Hossain and Do, 1992); and a surface diffusion model, that of poly(methylmethacrylate) surface and

Correspondence concerning this article should be addressed to H. Yoshida.

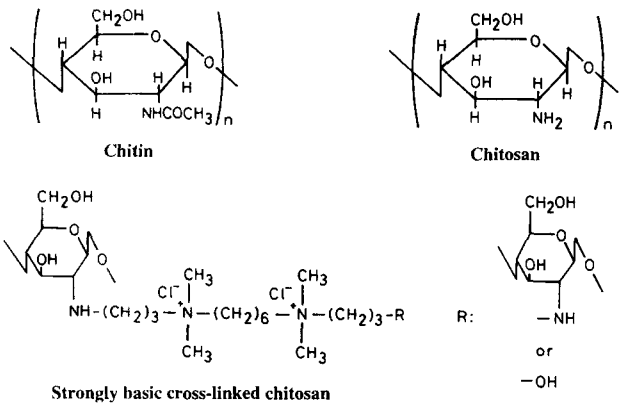

Figure 1. Unit molecular structures of chitin, chitosan, and strongly basic chitosan.

poly(dimethylsiloxane) surface (Tilton et al., 1990). Liapis (1990) assumed that in affinity chromatography, the surface diffusion is usually neglected, because there is strong interaction between the adsorbate and ligand and the pore diffusion is the rate controlling step. With other adsorbates such as ion exchangers, the interaction is not as strong as that for the adsorbent in affinity chromatography, so it may be necessary to consider both the surface and pore diffusion. In the present work, we apply parallel transport by surface and pore diffusions to intraparticle diffusion of a protein and present the experimental uptake curves for the adsorption of BSA on two different strongly basic chitosan beads, Chitopearl 2503 and Chitopearl 2507 (Fuji Spinning Co.), which are hard and highly porous ion exchangers. We determine intraparticle effective diffusivities from uptake curves measured for different bulk solution concentrations according to the homogeneous Fickian model and show the way in which the surface diffusivity and approximate pore diffusivity are determined using the experimental intraparticle effective diffusivities. We also calculate the pore diffusivities based on a pore diffusion model to find the region of pore diffusion control and the accurate pore diffusivity. The experimental uptake curves are compared with the parallel diffusion model using the Langmuir equilibrium isotherm, and the way in which the surface and pore diffusion affect the intraparticle diffusion of BSA is discussed.

Materials

We used Chitopearl 2503 and 2507 (Fuji Spinning Co., Japan), hereafter called Ch-2503 and Ch-2507, respectively. They are strongly basic chitosan. Figure 1 shows the unit molecular structures of original chitosan and the strongly basic chitosan. Chitosan is produced by deacetylation of chitin, which is a natural biopolymer found in the shells of arthropods such as lobsters, shrimps, and crabs. Since such arthropods are abundantly available, chitosan may be produced from them very cheaply, and as it is harmless to humans with no problems arising when it comes into contact with blood, ion exchangers or adsorbents made from chitosan may also have potential as separators of the proteins in blood and food. As chitosan is stable in alkaline solution but very soluble in acid solution and especially in organic acid solution, it was cross-linked to make an adsorbent with chemical proofs. The cross-linking reagent contains quaternary ammonium (strong base) and combines with the amino group of chitosan, as shown in Figure 1.

Table 1. Experimental Physical Properties of Strongly Basic Chitosan, Chitopearl 2503 and Chitopearl 2507 (Hard Gel)

	Ch-2507	Ch-2503
Particle Diameter* (μm)		
$d_{p,M}$	888.6	231.6
$d_{p,B}/d_p$	0.997	0.997
$d_{p,D}/d_p$	0.504	0.546
Standard Deviation of d_p	0.0479	0.0304
Ratio of Minor to Major Axis of d_p	0.979	0.981
Porosity	0.896	0.891
Pore Diameter (μm)	0.1-1	0.1-1
Density		
True (kg dry $\times$ m^{-3} dry)	1,475	1,468
Apparent (kg wet $\times$ m^{-3} wet)	1,124	1,049
Concentration of Quaternary Ammonium Group (Ion Exchange Capacity, Q) (eq m^{-3} Wet Resin)	478	163
Concentration of Amino Group (eq m^{-3} Wet Resin)	815	363
Water Content (wt. %)	79.4	84.7

* The particle diameters are arithmetic average values of 50 particles, respectively. d_p = particle diameter (free) in phosphate buffer solution (pH 6.9); $d_{p,B}$ = particle diameter saturated by BSA in phosphate buffer solution (pH 6.9); $d_{p,D}$ = dry particle diameter; $d_{p,M} = 0.5 \times (d_{p,B} + d_p)$.

Table 1 shows the experimental properties of Ch-2503 and Ch-2507. $d_{p,M}$ is an arithmetic mean diameter of 50 particles. The standard deviation of d_p is small. Since the ratio of minor to major axis of d_p is close to unity, the particles can be assumed to be spherical. There is little difference between the diameters of the particles which are free and saturated with BSA. The diameter of a wet particle is about twice that of a dry particle. The swelling of the strongly basic chitosan is much smaller than that of the dextran-type ion exchanger, QAE Sephadex A-50 (Yoshida et al., 1993). The porosities are about 0.9 and are quite large. Scanning electron microscopy (SEM) views have been investigated by Kawamura et al. (1993). Their studies showed that the pore diameter was about 0.1-1 μm. In spite of such large porosity and pore diameter, the resin particles are hard and do not become compressed in a column. The true densities are close to those of commercial ion-exchange resins for inorganic ions. As mentioned earlier, the amino groups of chitosan combine with the cross-linking reagent that has a quaternary ammonium group, but all the amino groups are not consumed by the reaction. Yoshida et al. (1994) determined not only the concentration of the quaternary ammonium groups, but also the concentration of the amino groups in the adsorbent phase for Ch-2503. Since we used a different lot of Ch-2503 than in the previous study, we measured them for the new lot of Ch-2503 and also for Ch-2507, as listed in Table 1. The concentration of quaternary ammonium groups in Ch-2507 is 2.9 times larger than that in Ch-2503. The concentration of amino groups in Ch-2507 is 2.2 times larger than that in Ch-2503. The concentration of quaternary ammonium groups in Ch-2507 is about 2.4 times larger than that in QAE Sephadex A-50 (Yoshida et al., 1993), but in Ch-2503 it is almost close to QAE Sephadex A-50.

Theory

Since the functional groups fixed on the surface of the pore in the chitosan particles are strongly basic, as shown in Figure 1, they are positively charged. When the pH of the protein solution is higher than the pI value of the protein, the protein

molecules are adsorbed by electrostatic attraction between the negatively charged protein molecules and the positively charged functional groups (Yoshida et al., 1993, 1994). As the interaction between the functional groups and the protein molecules is not very strong, we may assume the following:

(1) Surface and pore diffusion occur in parallel within the chitosan particle.

(2) Pore and surface diffusivities are constant during the adsorption process.

(3) The pore diameter and the void fraction of the chitosan particle are constant during the adsorption process.

(4) The concentration of the protein in the pore is in local equilibrium with the concentration of the protein adsorbed on the surface of the pore wall.

(5) The bulk phase concentration of the protein is constant during the adsorption process.

These assumptions lead to the following mass balance equation:

$$\epsilon\frac{\partial C}{\partial t}+\frac{\partial q}{\partial t}=D_P\epsilon\frac{1}{r^2}\frac{\partial}{\partial r}\left(r^2\frac{\partial C}{\partial r}\right)+D_S\frac{1}{r^2}\frac{\partial}{\partial r}\left(r^2\frac{\partial q}{\partial r}\right) \tag{1}$$

where C (kg/m^3) and q (kg/m^3 wet resin) are the liquid-phase concentration of the protein in the pore and the concentration of the protein adsorbed on the surface of the pore wall, respectively, ϵ is the void fraction of the pore, and D_P (m^2/s) and D_S (m^2/s) are the pore and surface diffusivities, respectively. Using dimensionless variables, we may transform Eq. 1 to Eq. 2:

$$\frac{\partial X}{\partial\tau_P}+\alpha\frac{\partial Y}{\partial\tau_P}=\frac{1}{\rho^2}\left(\rho^2\frac{\partial X}{\partial\rho}\right)+\frac{\beta}{\rho^2}\left(\rho^2\frac{\partial Y}{\partial\rho}\right) \tag{2}$$

where $X=C/C_0$, $\tau_P=D_pt/r_0^2$, $\rho=r/r_0$, $\alpha=q_0/\epsilon C_0$, and $\beta=\alpha D_S/D_P$. q_0 is the adsorbent-phase concentration which is in equilibrium with the concentration of protein in the bulk solution C_0.

The first and second terms of the righthand side of Eq. 2 show the contributions of the pore diffusion and surface diffusion, respectively. α and β are the important parameters in this parallel diffusion model. According to the definition of α, it means a distribution coefficient. β can be rewritten as follows:

$$\beta=\alpha\frac{D_S}{D_P}=\left(q_0\frac{15D_S}{r_0^2}\right)\Big/\left(\epsilon C_0\frac{15D_P}{r_0^2}\right)=\frac{k_sq_0}{k_P\epsilon C_0} \tag{3}$$

where $k_S(=15D_S/r_0^2)$ and $k_P(=15D_P/r_0^2)$ are the intraparticle mass-transfer coefficients based on the surface and pore diffusion, respectively. Equation 3 shows that β is the ratio of the rate of surface diffusion to that of pore diffusion. In other words, the degree of the contribution of the surface and pore diffusion should not be simply estimated from D_S/D_P, but must be judged from the value of β. There are two limiting cases: $\beta=0$ ($k_Sq_0=0$; pore diffusion control) and $\beta=\infty$ ($k_P\epsilon C_0=0$; surface diffusion control). When $\beta=0$, the second term of the righthand side of Eq. 2 disappears and the equation for the pore diffusion control is obtained. However, when $\beta=\infty$, Eq. 2 cannot be solved directly because the second term of the righthand side of Eq. 2 becomes infinite. Therefore, the first term of the righthand side of Eq. 1 is neglected and then transformed to Eq. 4:

$$\frac{\partial X}{\partial\tau_S}+\alpha\frac{\partial Y}{\partial\tau_S}=\frac{\alpha}{\rho^2}\left(\rho^2\frac{\partial Y}{\partial\rho}\right)\quad\text{(surface diffusion control, }\beta=\infty\text{)} \tag{4}$$

where $\tau_S=D_St/r_0^2$.

Applying the Langmuir isotherm expressed by Eq. 5:

$$Y=\frac{X}{R+(1-R)X} \tag{5}$$

and using assumption 4 we transform Eqs. 2 and 4 to Eqs. 6 and 7, respectively:

$$\left[\alpha+\frac{R}{\{1-(1-R)Y\}^2}\right]\frac{\partial Y}{\partial\tau_P}=\frac{1}{\rho^2}\frac{\partial}{\partial\rho}\left[\rho^2\frac{R}{\{1-(1-R)Y\}^2}\frac{\partial Y}{\partial\rho}\right]+\frac{\beta}{\rho^2}\frac{\partial}{\partial\rho}\left(\rho^2\frac{\partial Y}{\partial\rho}\right) \tag{6}$$

$$\left[\alpha+\frac{R}{\{1-(1-R)Y\}^2}\right]\frac{\partial Y}{\partial\tau_S}=\frac{\alpha}{\rho^2}\frac{\partial}{\partial\rho}\left(\rho^2\frac{\partial Y}{\partial\rho}\right)$$

(surface diffusion control, $\beta=\infty$) (7)

As mentioned above, Eq. 6 includes the pore diffusion control ($\beta=0$). The initial and boundary conditions are given by:

$$\begin{aligned}&\text{(I.C.)}\quad Y=0\ \text{ at }\ \tau_P=0\ \text{ or }\ \tau_S=0\\&\text{(B.C.)}\quad\frac{\partial Y}{\partial\rho}=0\ \text{ at }\ \rho=0\\&\qquad\quad Y=1\ \text{ at }\ \rho=1\end{aligned} \tag{8}$$

Assumption 5 gives the above boundary condition at the surface of the particle, that is, the adsorbent-phase concentration at the surface of the particle is constant.

Since we can determine experimentally only the change of the total concentration of the protein in the particle Q (kg/m^3 wet resin) with time, we define the fractional attainment of equilibrium F by Eq. 10:

$$Q=q+\epsilon C \tag{9}$$

$$F=\frac{3\int_0^{r_0}Qr^2dr}{Q_0}=\frac{3\left[\alpha\int_0^1Y\rho^2d\rho+\int_0^1X\rho^2d\rho\right]}{\alpha+1} \tag{10}$$

where $Q_0=q_0+\epsilon C_0$. Since Eqs. 6 and 7 are nonlinear differential equations, they are transformed into finite difference equations and solved numerically, and the solutions of the change of F with time are obtained.

When $\alpha\ (=q_0/\epsilon C_0)=\infty$, the concentration of the protein on the pore wall is very much larger than that in the pore. Therefore, the pore diffusion is negligible and the surface diffusion is the rate controlling step. This is confirmed by substituting $\alpha=\infty$ into Eq. 2. Dividing both sides of Eq. 2 by α and using the relation $\beta=\alpha D_S/D_P$, the terms related to the

concentration of protein in the pore disappear and Eq. 11 is derived:

$$\frac{\partial Y}{\partial \tau_S}=\frac{1}{\rho^2}\left(\rho^2\frac{\partial Y}{\partial \rho}\right) \quad \text{(surface diffusion control, } \alpha=\infty) \tag{11}$$

Equation 10 is also reduced to Eq. 12 when $\alpha=\infty$:

$$F=\frac{3\int_0^{r_0} Qr^2dr}{Q_0}=3\int_0^1 Y\rho^2 d\rho \tag{12}$$

Equation 11 has been normally used as the basic equation for the surface diffusion model. The solution under the initial and boundary conditions, Eq. 8, is given by Eq. 13 (Carslaw and Jaeger, 1959):

$$F=1-\frac{6}{\pi^2}\sum_{n=1}^{\infty}\frac{1}{n^2}\exp(-n^2\pi^2\tau_s) \tag{13}$$

It should be stressed that Eq. 11 can be used only when $\alpha=\infty$. When α is relatively large but not infinite, the surface diffusion control expressed by Eq. 11 can be used only when $\beta\gg1$. Otherwise, even if α is large, Eq. 6 must be solved. These are discussed in detail in the discussion section. In addition, the theoretical equations presented here can be applied not only for adsorption of proteins but also for adsorption of small molecules on general adsorbents.

Experimental

Before measuring the equilibrium isotherms and kinetic data, the strongly basic chitosan particles were packed in a column and were thoroughly washed with 100 mol/m^3 NaOH aqueous solution. As the chitosan resin has quaternary ammonium groups, as shown in Figure 1, that is, it is a strongly basic ion exchanger, any counter ions (anions), which neutralize the fixed quaternary ammonium groups (plus charges) in the resin phase, are exchanged for OH^- ions by flowing NaOH aqueous solution. Thereafter, the bed was washed with deionized distilled water. The OH^--form chitosan particles were transformed to a phosphate form by using a 6.975 eq/m^3 phosphate buffer of pH 6.9 ($Na_2HPO_4+NaH_2PO_4$). The particles were kept in the buffer solution and not dried because the adsorption of proteins is reduced when they are dried. Just before measuring the equilibria or kinetic data, the solution around the particles was removed using a centrifugal filter (Sanyo Rikagaku-Kiki Seisakusho) at 5,000 rpm for 4 minutes, and the particles were weighed.

We measured the equilibrium isotherms for adsorption of BSA by the batch method. The pH of the BSA solution was adjusted to 6.9 using phosphate buffer as mentioned above. The strongly basic chitosan particles were added to the BSA solution in a syringe vial. Just before using the syringe vials, they were sterilized with 75% ethanol aqueous solution and then dried. The resin particles were weighed and put into the syringe vial. Thereafter, the vial was filled with BSA solution using Pipetman (Gilson) by which the volume of the solution was determined. There was no air in the syringe vial. The syringe vials were rotated gently. The solution was mixed by

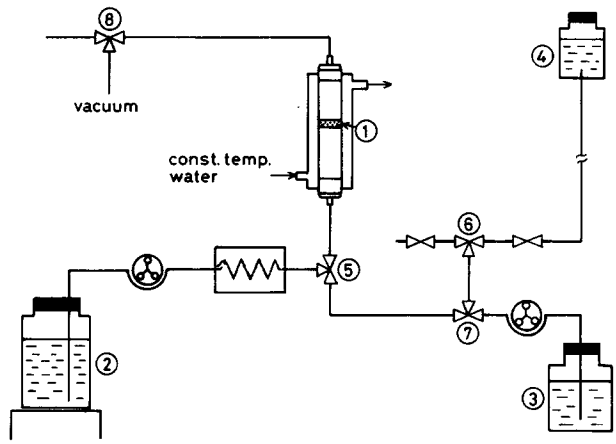

Figure 2. Experimental apparatus of shallow bed method.

(1) Shallow bed; (2) BSA solution (pH = 6.9); (3) NaCl solution (200 mol/m^3); (4) buffer solution (pH = 6.9), 5-8; three-way cock.

the motion of the resin particles in the vessel. We measured the amount of BSA adsorbed on the resin after 4 to 7 days. We confimed that there was no difference between the results for 5 to 7 days. Then we contacted the resin and BSA solution for 5 days. We have to stress here that since air did not exist in the syringe vial in this experimental study, BSA was not denatured. This is what we found as an important experimental technique to restrain the denaturation of a protein for a relatively long period. If air was in the vial, even the volume is much smaller than the solution, and the denaturation of BSA was of course a serious problem. We confirmed that the adsorption of BSA on the wall of the syringe vial was negligibly small by blank test. The adsorbent-phase concentration of BSA was calculated according to Eq. 14:

$$q^*=\frac{(C_I-C^*)V}{W} \tag{14}$$

where C_I and C^* are the initial concentration and equilibrium concentration of BSA in the liquid phase (kg/m^3), respectively. q^* denotes the adsorbent-phase equilibrium concentration of BSA (kg/m^3 wet adsorbent), V shows the volume of the solution (m^3), and W represents the volume of the wet adsorbent particles (m^3).

We measured the kinetic data by the shallow bed method and the batch method (mixing vessel). Figure 2 shows the experimental apparatus used for the shallow bed method. In this experimental study, we improved the shallow bed method, which we had previously used for investigating the diffusion mechanisms in ternary ion-exchange systems (Yoshida and Kataoka, 1987). The column has a jacket to maintain the bed at a constant temperature. The inside diameter of the column was 1 cm. The strongly basic chitosan particles were placed in the column. The shallow bed was one or two particle layers to prevent change in the bulk solution concentration. The buffer solution of pH 6.9, which was the same pH as the BSA solution, flowed through the column from tank 4 (see Figure 2) until the resin particles reached equilibrium with the buffer. Thereafter, the BSA solution of pH 6.9 was fed into the column from tank 2 for various periods of time. Then the buffer

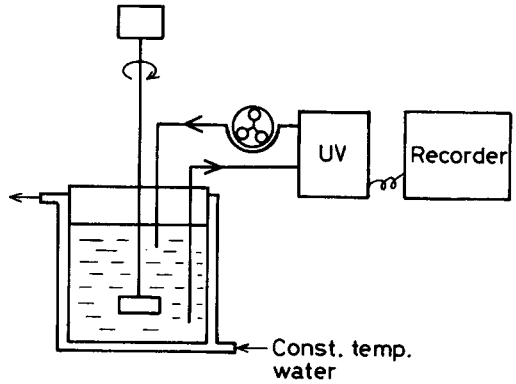

Figure 3. Experimental apparatus of batch method.

solution was instantaneously supplied from tank 4, and the bed was washed for about two to three seconds. Since the BSA solution must be completely removed quickly from the void of the bed and the tube, we used a vacuum pump to flow the buffer solution at a high speed. The BSA in the resin phase was then desorbed by flowing aqueous NaCl solution of 200 mol/m^3 from tank 3. We analyzed the solution for BSA with a Shimadzu UV-Visible Recording Spectrophotometer UV-260 ($\lambda = 278.0$ nm) and the mean adsorbent phase concentration of BSA was determined according to Eq. 15:

$$\overline{Q} = \frac{C_e V_e}{W} \tag{15}$$

where $\overline{Q}$ (kg/m^3 wet resin) and C_e (kg/m^3) are the mean concentration of BSA in the resin phase and the concentration of BSA in the eluate, respectively. V_e (m^3) and W (m^3 wet resin) denote the volume of the eluate and the resin particles, respectively.

We also measured the kinetic data by the batch method. Figure 3 shows the experimental apparatus. The mixing vessel was 10 cm in diameter and 14 cm deep with four baffle plates and a jacket. 400 cm^3 of BSA solution of pH 6.9 was stirred using a flat paddle (3 cm × 1 cm) in the vessel. After the solution reached the constant temperature of 298 K, the strongly basic chitosan particles were added to the solution. BSA was analyzed continuously with a Shimadzu UV-VIS Spectrophotometric detector SPD-6AV ($\lambda = 278.0$ nm). The mean adsorbent phase concentration of BSA was determined from Eq. 16:

$$\overline{Q} = \frac{(C_I - C_0)V}{W} \tag{16}$$

C_0 denotes the bulk phase concentration of BSA (kg/m^3).

All the experiments were carried out at 298 K.

Results

Yoshida et al. (1994) have determined the detailed experimental equilibrium isotherms for the adsorption of BSA on Ch-2503. They showed that the isotherm was strongly affected by pH. When the pH was 6.9, the initial concentration of BSA did not affect the isotherm. The saturation capacity for adsorption of BSA on Ch-2503 was 1.3 ~ 2.2 times larger than DEAE Sephrose Fast Flow (hard gel, Pharmacia Fine Chemicals). BSA could be desorbed completely using a 200 mol/m^3 aqueous NaCl solution. Since in this study we used a different lot of Ch-2503 than in our previous study (Yoshida et al., 1994), we measured the equilibrium isotherm for adsorption of BSA on the new lot of Ch-2503 at pH 6.9. We also measured the isotherm for Ch-2507. The isotherms were independent of the initial concentration of BSA. The data were correlated reasonably well by the Langmuir equation (Eq. 17):

$$q = \frac{Kq_\infty C}{1 + KC} \tag{17}$$

The experimental Langmuir coefficients are listed in Table 2. The equilibrium constant K (m^3/kg) and saturation capacity q_∞ (kg/m^3 wet adsorbent) for Ch-2503 are a little larger than those for Ch-2507.

Figure 4 shows the experimental uptake curves for the adsorption of BSA on Ch-2507 and Ch-2503 when the concentration of BSA in the bulk solution, C_0, was 1 kg/m^3. The experimental conditions are given in Table 2. Since the diameter of Ch-2507 particles is about 3.8 times larger than Ch-2503 particles (see Table 1), the adsorption rate of BSA on Ch-2507 is slower than on Ch-2503. The uptake data for Ch-2507 were determined by the shallow bed method. In order to confirm whether the adsorption rate is controlled by the intraparticle diffusion or not, we measured the data for three different flow rates ($Re = 2.3$, 5.3, and 7.3) with a bulk phase concentration of $C_0 = 1$ kg/m^3. Since the flow rate did not affect the adsorption rate, as shown in Figure 4, the intraparticle diffusion is the rate controlling step in $Re \geq 2.3$. Therefore, the other

Table 2. Experimental Conditions for Uptake Curve and Model Parameters for Calculating Theoretical Uptake Curve (298 K and pH 6.9)

C_0 kg·m^{-3}	q_0 kg·m^{-3}	q_∞ kg·m^{-3}	K m^3·kg^{-1}	R	$D_S \times 10^{13}$ m^2·s^{-1}	$D_P \times 10^{13}$ m^2·s^{-1}	α	β
Ch-2507 (Shallow Bed Method)								
0.3	133	181	9.23	0.265	0.47	270	495	0.875
1	163			0.0978			182	0.322
2	172			0.0514			95.8	0.169
3	175			0.0349			65.0	0.115
Ch-2503 (Batch Method)								
0.456	160	190	11.8	0.157	2.4	100	392	9.54
0.956	175			0.0814			204	4.95
1.46	180			0.0549			137	3.34
2.40	184			0.0341			85.2	2.07
2.96	185			0.0283			70.9	1.72

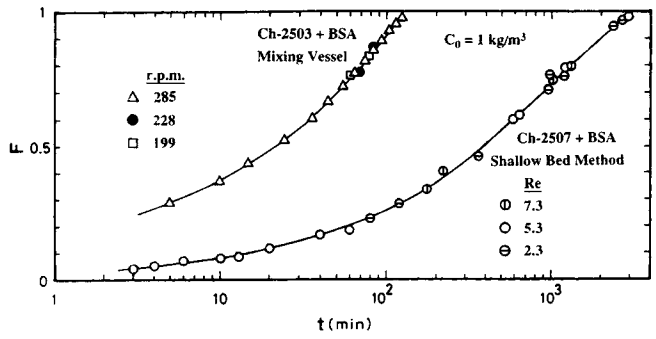

Figure 4. Comparison between experimental uptake curves for adsorption of BSA on Ch-2503 (batch method) and Ch-2507 (shallow bed method).

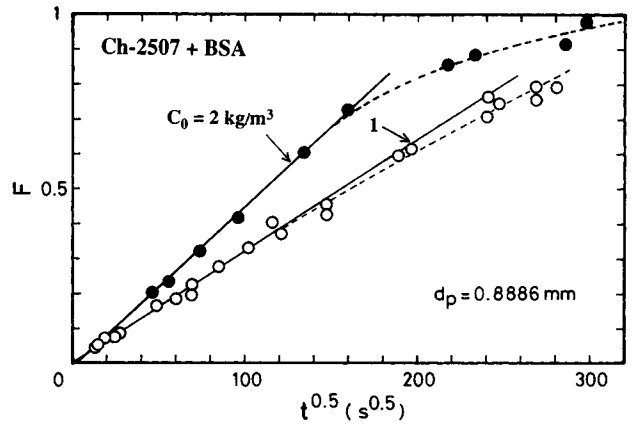

Figure 5. Plots of uptake data for adsorption of BSA on Ch-2507 according to Eq. 21.

BSA solutions of $C_0 = 0.3$, 2, and 3 kg/m³ (see Table 2) were flowed through the bed under $Re = 7.3$. The experimental uptake curves for adsorption of the BSA on Ch-2503 were determined by the batch method. We confirmed that when the rotating speed of the paddle was larger than 199 rpm, the liquid film diffusion resistance surrounding the particles could be neglected. The uptake curves shown in Figure 4 and in Table 2 were measured at a speed of 285 rpm. In order to satisfy the boundary condition of Eq. 8, in other words, to maintain a constant bulk phase concentration during the adsorption process, the difference between the initial and final concentration of BSA in the bulk phase was kept within 10~15% of the initial concentration. The bulk phase concentration C_0 (kg/m³) in the batch method (see Table 2 and Figure 4) is the average value of the initial and final concentration of BSA in the mixing vessel.

The adsorption rate increased as the bulk phase concentration of BSA; C_0 increased as mentioned below. These results suggest that pore diffusion resistance may exist in the intraparticle diffusion.

Discussion

Intraparticle effective diffusivity

To determine the surface diffusivity D_S (m²/s) and pore diffusivity D_P (m²/s) based on the parallel diffusion model, we calculated the effective diffusivities for the homogeneous model. Assuming Fickian diffusion with a constant effective diffusivity, the mass balance equation in the particle is given by Eq. 18:

$$\frac{\partial Q}{\partial t} = D_{\text{eff}} \frac{1}{r^2} \frac{\partial}{\partial r}\left(r^2 \frac{\partial Q}{\partial r}\right) \tag{18}$$

Q as defined by Eq. 9 was used because we measured the change of the total concentrations of the protein in the pore solution and the protein adsorbed on pore wall with time. The initial and boundary conditions are given by:

$$\text{(I.C.)} \quad Q = 0 \quad \text{at} \quad t = 0$$

$$\text{(B.C.)} \quad \frac{\partial Q}{\partial \rho} = 0 \quad \text{at} \quad r = 0$$

$$Q = Q_0 (= q_0 + \epsilon C_0) \quad \text{at} \quad r = r_0 \tag{19}$$

The solution is given by Eq. 20 (Carslaw and Jaeger, 1959):

$$F = \frac{3\int_0^{r_0} Qr^2 dr}{Q_0} = \frac{3\left[\alpha \int_0^1 Y\rho^2 d\rho + \int_0^1 X\rho^2 d\rho\right]}{\alpha + 1}$$

$$= 1 - \frac{6}{\pi^2} \sum_{n=1}^{\infty} \frac{1}{n^2} \exp\left(-n^2\pi^2 \frac{D_{\text{eff}} t}{r_0^2}\right) \tag{20}$$

The corresponding solution for shorter times is given by Eq. 21 (Crank, 1975):

$$F = \frac{3\int_0^{r_0} Qr^2 dr}{Q_0} = 6\left(\frac{D_{\text{eff}} t}{r_0^2}\right)^{1/2}$$

$$\times \left\{\pi^{-1/2} + 2\sum_{n=1}^{\infty} \text{ierfc} \frac{nr_0}{\sqrt{D_{\text{eff}} t}}\right\} - 3\left(\frac{D_{\text{eff}} t}{r_0^2}\right) \tag{21}$$

Equation 21 shows that F is directly proportional to $t^{1/2}$ for shorter times. Figure 5 shows examples of the plots of F vs. $t^{1/2}$ for Ch-2507. The data can be correlated by straight lines when $t^{1/2}$ is smaller than about 100. The values of D_{eff} were determined from the slopes of the straight lines, which are equal to $6(D_{\text{eff}}/r_0^2\pi)^{1/2}$. Table 3 lists the experimental values

Table 3. Experimental Intraparticle Effective Diffusivity of BSA in Ch-2503 (Hard Gel), CH-2507 (Hard Gel), and DEAE Sephadex A-50 (Soft Gel) at 298 K and pH 6.9

Ch-2507		Ch-2503		DEAE Sephadex A-50*	
C_0 kg·m⁻³	$D_{\text{eff}} \times 10^{13}$ m²·s⁻¹	C_0 kg·m⁻³	$D_{\text{eff}} \times 10^{13}$ m²·s⁻¹	C_0 kg·m⁻³	$D_{\text{eff}} \times 10^{13}$ m²·s⁻¹
0.3	1.0	0.456	2.7	1.2	21
1	1.9	0.956	3.3		
2	3.7	1.46	3.6		
3	4.6	2.40	4.5		
		2.91	4.5		

*Tsou and Graham (1985).

of D_{eff} for BSA for Ch-2503, Ch-2507, and DEAE Sephadex A-50 (Tsou and Graham, 1985). D_{eff} increases as the bulk phase concentration of BSA (C_0) increases. The values of D_{eff} for CH-2503 are larger than those for Ch-2507, especially when C_0 is small. However, since they are smaller than those of the soft gel DEAE Sephadex A-50, strongly basic chitosan resins (hard gel) need to be improved in order to increase D_{eff}.

Surface diffusivity and approximate pore diffusivity

When the surface diffusion is the rate-controlling step and $\alpha\ (=q_0/\epsilon C_0)=\infty$, Eq. 11 is rewritten into Eq. 22:

$$\frac{\partial q}{\partial t}=D_S\frac{1}{r^2}\frac{\partial}{\partial r}\left(r^2\frac{\partial q}{\partial r}\right) \tag{22}$$

When $\alpha=\infty$ ($q_0 \gg C_0$), Q becomes equal to q according to the definition, Eq. 9, and then Eq. 18 is reduced to Eq. 23:

$$\frac{\partial q}{\partial t}=D_{\text{eff}}\frac{1}{r^2}\frac{\partial}{\partial r}\left(r^2\frac{\partial q}{\partial r}\right) \tag{23}$$

From Eqs. 22 and 23, the effective diffusivity for $\alpha=\infty$ (or $1/\alpha=0$) gives the surface diffusivity. On the other hand, Eq. 24 is derived from the relation between the fluxes based on the parallel diffusion model and the Fickian model:

$$D_{\text{eff}}\left(1+\epsilon\frac{dC}{dq}\right)=D_S+\epsilon D_P\frac{dC}{dq} \tag{24}$$

Equation 24 has been given by Yoshida et al. (1991) for adsorption of dye molecules on a porous cellulose membrane. When $dC/dq \ll 1$, Eq. 24 is reduced to Eq. 25:

$$D_{\text{eff}}=D_S+\epsilon D_P\frac{dC}{dq} \tag{25}$$

Takeuchi et al. (1984) have shown that there exist surface and pore diffusion resistances for the adsorption of tetrahydrofuran vapor on activated carbon particles. Their measurements were made under steady-state conditions in a diaphragm cell. They correlated their experimental effective diffusivities according to Eq. 26, which was derived by substituting $dC/dq=\Delta C/\Delta q$ into Eq. 25, and obtained the surface and pore diffusivities from the intercept and slope, respectively:

$$D_{\text{eff}}=D_S+\epsilon D_P\frac{\Delta C}{\Delta q} \tag{26}$$

Costa et al. (1985) measured intraparticle diffusivities from uptake data for the adsorption of several hydrocarbon gases on activated carbon particles by changing the bulk pressure differentially. The successive amounts of adsorbate that were added were always small enough that the adsorption isotherm could be considered linear in the concentration range examined. They plotted the intraparticle diffusivities vs. the dimensionless mean slope, K^*, of the equilibrium isotherm in the concentration range of each experiment. The slope and the intercept gave the pore and surface diffusivities according to Eq. 27:

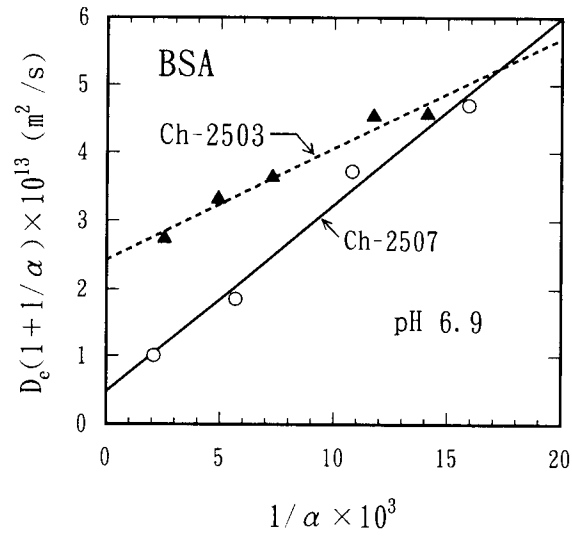

Figure 6. Plots of intraparticle effective diffusivities based on Eq. 28.

$$D_{\text{eff}}=D_P+K^*D_S \tag{27}$$

Since, in our experimental method, dC/dq may be a function of both time and the position within a particle, it cannot be determined from the equilibrium isotherm only. By taking $dC/dq=C_0/q_0$ as an approximation, Eq. 24 is transformed into Eq. 28:

$$D_{\text{eff}}\left(1+\frac{1}{\alpha}\right)=D_S+D_{Pa}\frac{1}{\alpha} \tag{28}$$

The above approximation is correct for a linear isotherm system, but even in a nonlinear isotherm system, the approximation gives integral mean value of dC/dq from $q=0$ to q_0 ($C=0$ to C_0):

$$\frac{1}{q_0}\int_0^{q_0}\frac{dC}{dq}dq=\frac{C_0}{q_0} \tag{29}$$

When $1/\alpha\ (=\epsilon C_0/q_0)\to 0$ in Eq. 28, D_{eff} approaches D_S. However, the value of the slope of the plots of the lefthand side vs. $1/\alpha$ may not give an accurate pore diffusivity because of the approximation of $dC/dq=C_0/q_0$. Therefore, the slope is written as D_{Pa} which stands for the approximate pore diffusivity. Only when the isotherm is linear, D_{Pa} is equal to D_P. If the plots based on Eq. 28 are linear and the intercept is zero ($D_S=0$), the pore diffusion is the rate controlling step. If the slope of the plots is zero ($D_{Pa}=0$), the surface diffusion is the rate controlling step. Otherwise, parallel transport by surface and pore diffusion may exist.

Figure 6 shows the plot of the experimental effective diffusivities based on Eq. 28. The experimental data for Chitopearl 2507 ($d_p=0.8886$ mm) and Chitopearl 2503 ($d_p=0.2316$ mm) can be correlated well by the straight solid and broken lines, respectively. The value of the intercept of the straight line gives the surface diffusivity D_S and the slope of the line provides the approximate pore diffusivity D_{Pa}, which are listed in Table 4. The value of D_S for Ch-2503 is about 5.2 times

Table 4. Surface Diffusivity, Pore Diffusivity, and Liquid Phase Diffusivity of BSA at 298 K and pH 6.9

Resin	D_S ($m^2 \cdot s^{-1}$)	D_{Pa} ($m^2 \cdot s^{-1}$)	D_P ($m^2 \cdot s^{-1}$)	D_P/D_L
Ch-2507	0.47×10^{-13}	2.8×10^{-11}	2.7×10^{-11}	0.39
Ch-2503	2.4×10^{-13}	1.6×10^{-11}	1.0×10^{-11}	0.15

* Liquid phase diffusivity of BSA, D_L was 6.84×10^{-11} $m^2 \cdot s^{-1}$, which was calculated from the data presented by Tyn and Guesk (1990) at 293 K and Eq. 32.

larger than that for Ch-2507. On the other hand, the value of D_{Pa} for Ch-2503 is about 60% of the value for Ch-2507.

Pore diffusivity based on shrinking core model

As mentioned earlier, when the equilibrium isotherm is not linear but favorable, as it is in our adsorption system (see the values of K in Table 2), D_{Pa} does not give an accurate pore diffusivity. Therefore, we determined the pore diffusivity by assuming pore diffusion control. The values of the dimensionless Langmuir equilibrium constant R were calculated from Eq. 30 and are listed in Table 2.

$$R = \frac{1}{1 + KC_0} \tag{30}$$

When $R < 0.1$, the equilibrium isotherm may be assumed to be rectangular. Since Table 2 shows that the values of R are smaller than 0.1 when $C_0 \leq 1$ kg/m^3 for Ch-2507 and $C_0 \leq 0.956$ kg/m^3 for Ch-2503, respectively, we applied the well-known "shrinking core" model based on the pore diffusion control with a rectangular equilibrium isotherm. The solution for the uptake curve under these conditions was obtained by Yagi and Kunii (1953) and has since been applied in several different contexts, for example, Weistz and Goodwin (1963), Levenspiel (1966), Wen (1968). The solution is:

$$\frac{6\epsilon D_P' C_0}{q_0 r_0^2} t = 1 + 2(1-F) - 3(1-F)^{2/3} \tag{31}$$

which provides a simple implicit expression for the dimensionless uptake curve. D_P' is the pore diffusivity based on the pore diffusion control and the shrinking core model. Figure 7

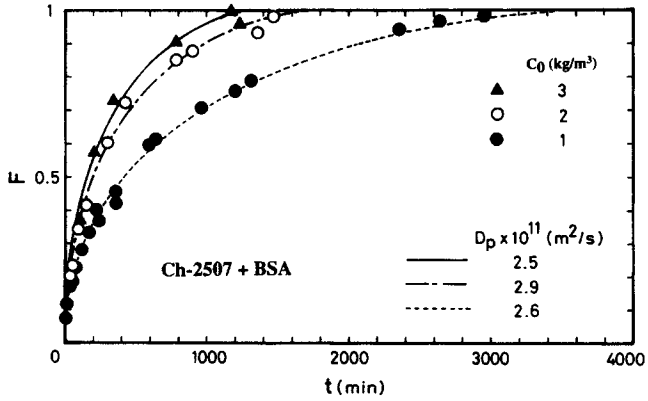

Figure 7. Comparison between uptake data for adsorption of BSA on Ch-2507 and Eq. 31.

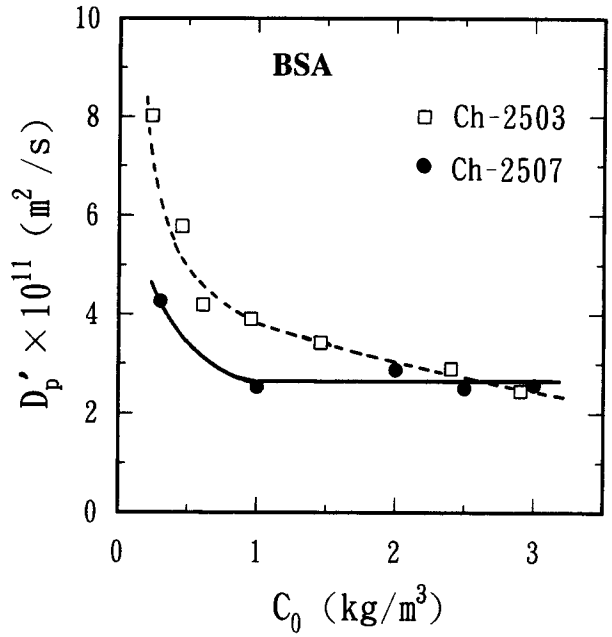

Figure 8. Effect of bulk phase concentration (C_0) on pore diffusivity (D_P') determined using Eq. 31.

shows a comparison between the experimental uptake data for the adsorption of BSA on Ch-2507 and Eq. 31. The theoretical lines agree reasonably well with the data. The values of D_P' were determined by matching the uptake data with Eq. 31. Equation 31 agreed reasonably well with the uptake data for Ch-2503 too.

Yoshida et al. (1991) have measured the uptake curves and the concentration profiles for the adsorption of dyestuffs on cellulose membranes and proved that the experimental uptake curves agree with any model but the experimental concentration profiles agree with only a reasonable model. In our study, it is impossible to measure the intraparticle concentration profile of BSA. According to Yoshida et al.'s investigation (1991), we must consider that the D_P' determined by matching the uptake data with Eq. 31 is affected by not only the pore diffusion but also by other diffusion mechanisms even if the uptake data agree well with Eq. 31. If D_P' decreases while the concentration of BSA in the bulk solution (C_0) increases and reaches a constant value, we can conclude that the pore diffusion is the rate controlling step in the constant pore diffusivity region. In the region where D_P' is larger than the constant value, pore diffusion occurs in parallel with other diffusions such as surface diffusion when $R < 0.1$. When $R > 0.1$, that is, the concentration of the bulk solution is low, the deviation of D_P' from the constant value may be caused not only by the existence of parallel diffusion but also by the deviation from the assumption of rectangular isotherm.

Figure 8 shows the effect of the bulk phase concentration of BSA, C_0 on D_P' determined using Eq. 31. In the case of Ch-2507, D_P' decreases as C_0 in $C_0 < 1$ kg/m^3 increases and is almost constant in 1 kg/m$^3 \leq C_0 \leq 3$ kg/m^3. The average value of D_P' in $C_0 \geq 1$ kg/m^3 is 2.7×10^{-11} m^2/s. From the above discussion, pore diffusion is the rate controlling step in $C_0 \geq 1$ kg/m^3 and the constant value 2.7×10^{-11} m^2/s may give the accurate pore diffusivity D_P. In Ch-2503, D_P' decreases as the C_0 increases in $C_0 \leq 3$ kg/m^3. The value of R for Ch-2503 is similar to that

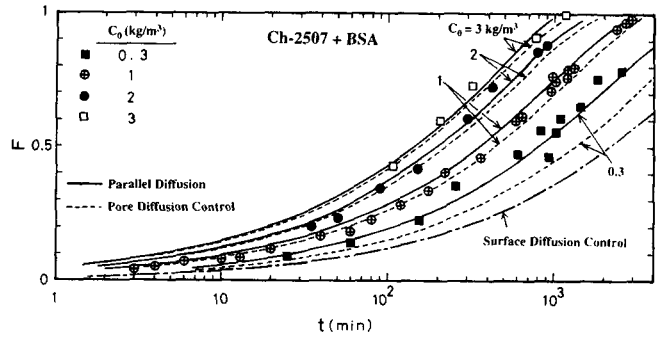

Figure 9. Experimental and theoretical uptake curves for adsorption of BSA on Ch-2507.

—— Parallel diffusion model, Eq. 6, ($D_S = 0.47 \times 10^{-13}$ m²/s and $D_P = 2.7 \times 10^{-11}$ m²/s); ------ pore diffusion control, Eq. 6 and $\beta = 0$, ($D_P = 2.7 \times 10^{-11}$ m²/s); —·—·— surface diffusion control, Eq. 13, ($D_S = 0.47 \times 10^{-13}$ m²/s).

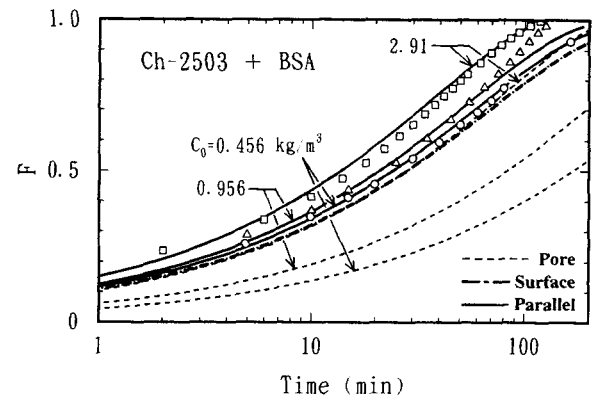

Figure 10. Experimental and theoretical uptake curves for adsorption of BSA on Ch-2503.

—— Parallel diffusion model, Eq. 6, ($D_S = 2.4 \times 10^{-13}$ m²/s and $D_P = 1.0 \times 10^{-11}$ m²/s); ------ pore diffusion control, Eq. 6 and $\beta = 0$, ($D_P = 1.0 \times 10^{-11}$ m²/s); —·—·— surface diffusion control, Eq. 13, ($D_S = 2.4 \times 10^{-13}$ m²/s). □, $C_0 = 2.91$ kg/m³; △, $C_0 = 0.956$ kg/m³; ○, $C_0 = 0.456$ kg/m³.

for Ch-2507 as shown in Table 2, namely, when $C_0 \geq 1$ kg/m³, $R < 0.1$ for both resins. As D_P' for Ch-2507 is constant when $C_0 \geq 1$ kg/m³, the assumption of the rectangular isotherm can be used for CH-2503 too. The reason why D_P' does not approach to a constant value in $C_0 \geq 1$ kg/m³ may be caused by neglecting the effect of the surface diffusion. Therefore, the accurate pore diffusivity D_P for Ch-2503 cannot be determined from the data of D_P'. This is reasonable, because the D_S for Ch-2503 is about 5.2 times larger than that for Ch-2507 (see Figure 6) and the effect of the surface diffusion in Ch-2503 may be more significant than in Ch-2507.

Parallel transport by surface and pore diffusion

Since the surface diffusivity D_S and the pore diffusivity D_P for Ch-2507 were determined above, we calculated the theoretical uptake curves for Ch-2507 based on the parallel transport by the surface and pore diffusions (Eq. 6). The dimensionless parameters used for the calculation of Eq. 6 are given in Table 2. The theoretical lines are shown by the solid lines in Figure 9, and agree reasonably well with the data. We also calculated the theoretical lines for the pore diffusion control (broken line) and surface diffusion control (chain line). The theoretical lines for the pore diffusion control were obtained by setting $\beta = 0$ ($D_S = 0$) in Eq. 6 and using the same pore diffusivity as the one used for the calculation of the parallel diffusion model ($D_P = 2.7 \times 10^{-11}$ m²/s). Since we proved that when $1/\alpha$ ($= \epsilon C_0/q_0$) $\rightarrow 0 (\alpha \rightarrow \infty)$ (see Eq. 28 and Figure 6), the surface diffusion is the rate controlling step. The theoretical line of the surface diffusion control was determined according to Eq. 11, using the same surface diffusivity as the one for the parallel diffusion model ($D_S = 4.7 \times 10^{-14}$ m²/s). Figure 9 shows that as deviation from the surface diffusion model (chain line) increases, the bulk phase concentration C_0 increases (that is, as α and β decrease). Even when $C_0 = 0.3$ kg/m³ ($\alpha = 495$, $\beta = \alpha D_S/D_P = 0.875$), there is a large difference between the data and the theoretical line for the surface diffusion control. The difference between the theoretical lines of the parallel diffusion model (solid line) and pore diffusion model (broken line) decreases as C_0 increases. Since when $C_0 \geq 1$ kg/m³ ($\alpha \leq 182$, $\beta \leq 0.322$) the difference is small, we can assume that the pore diffusion is the rate controlling step in this region. The fact that the D_P' for Ch-2507 was constant (2.7×10^{-11} m²/s) in $C_0 \geq 1$ kg/m³ (see Figure 8) supports the above results.

Figure 10 shows a comparison between the uptake data for Ch-2503 and the theoretical lines for the parallel diffusion model, pore diffusion model, and surface diffusion model. The solid lines are the theoretical lines for the parallel diffusion model (Eq. 6), which were calculated using the dimensionless parameters given in Table 2. The value of D_S ($= 2.4 \times 10^{-13}$ m²/s) was determined from the intercept of the plot in Figure 6 as mentioned earlier. Since the D_P' for Ch-2503 did not reach the constant value of this experimental condition (see Figure 8), we determined the value of D_P ($= 1.0 \times 10^{-11}$ m²/s) by matching Eq. 6 with the data. The solid lines for three different bulk phase concentrations agree reasonably well with the data. The chain line shows the surface diffusion model (Eq. 11) using $D_S = 2.4 \times 10^{-13}$ m²/s. The uptake data for $C_0 = 0.456$ kg/m³ ($\alpha = 392$, $\beta = 9.54$) are close to the theoretical line for the surface diffusion model. The data deviates from the surface diffusion model as the bulk phase concentration increases because the contribution of the pore diffusion increases as the bulk phase concentration increases (that is, as α and β decrease). The broken lines show the theoretical lines for the pore diffusion model (Eq. 6, $\beta = 0$) using the same D_P as the one calculated for the parallel diffusion model. The uptake data are much faster than those predicted from the pore diffusion because the contribution of the surface diffusion is significant.

In Ch-2507, the uptake data deviated from the surface diffusion model even when $C_0 = 0.3$ kg/m³ ($\alpha = 495$, $\beta = 0.875$). The surface diffusion in Ch-2503 is more significant than in Ch-2507 because the D_S value for Ch-2503 is about 5.2 times larger than that for Ch-2507. This may be caused by the fact that the concentration of quaternary ammonium group in the solid phase of Ch-2507 is about three times larger than that of Ch-2503. BSA molecules are negatively charged at pH 6.9 in this experimental condition, because the isoelectric point of BSA is about 4.8 (Wallevik, 1973; Evanston and Deutsch, 1978). The electrostatic attraction between a negatively charged BSA molecule and positively charged fixed groups in Ch-2507 is therefore stronger than that in Ch-2503, and it is more

difficult for the BSA molecule in Ch-2507 to move on the surface than in Ch-2503.

Table 2 shows that the values of α ($=q_0/\epsilon C_0$) for Ch-2503 and Ch-2507 are almost the same when C_0 is the same. On the other hand, their β ($=\alpha D_S/D_P$) are relatively different. As mentioned in the section on theory, there are two limiting cases, $\beta=0$ (pore diffusion control) and $\beta=\infty$ (surface diffusion control). From Figures 9 and 10, and Table 2, when $\beta>10$, we can assume the surface diffusion is the rate controlling step. When $\beta<0.3$, the pore diffusion model can be used approximately. When $0.3<\beta<10$, the parallel transport by the surface and pore diffusions should be considered.

Table 4 summarizes the diffusivities obtained in this study. The D_P value is smaller than D_{Pa} which is the slope of the plot in Figure 6. In Ch-2507, the pore diffusion is more significant than the surface diffusion, and the D_P is about 96% of the D_{Pa}. On the other hand, in Ch-2503 surface diffusion is more significant than the pore diffusion and the D_P is about 61% of the D_{Pa}. The reason why D_P is almost the same as D_{Pa} when pore diffusion is more significant than the surface diffusion and the D_P is relatively smaller than the D_{Pa} when the surface diffusion is more significant than the pore diffusion still is not clear.

We calculated the diffusivity ratios of the pore diffusivity to the liquid phase diffusivity, D_P/D_L which are given in Table 4. Several experimental values of D_L for BSA at 293 K have been summarized by Tyn and Gusek (1990). Those values are about the same with an average value of 5.98×10^{-11} m^2/s. Since our experiments were carried out at 298 K, we estimated the value of D_L for BSA at 298 K using the above average value at 293 K and Eq. 32:

$$\frac{\mu D_L}{T}=\text{constant} \tag{32}$$

The porosity ϵ of the chitosan particle is 0.896 (Table 1). Suzuki (1990) has summarized a number of the data, which showed the effect of the porosity on the diffusivity ratio for normal small molecules. According to the figure which he presented, when ϵ is about 0.9, the diffusivity ratio is $0.2\sim0.8$. Therefore, the values of D_P for BSA in Ch-2507 and Ch-2503 determined in this study may be reasonable.

The parallel diffusion model was applied for strongly basic chitosan ion exchangers in this study. The theory and the procedure for determining the surface and pore diffusivities presented here may be used generally for the intraparticle mass transfer of not only proteins but also any adsorbates in porous adsorbents. If the plot based on Eq. 28 cannot be correlated by a straight line, other diffusion mechanism should be considered.

Acknowledgment

This research was partly supported by grant in aid for Scientific Research No. 63550715 from the Ministry of Education, Culture and Science, Japan.

Notation

C = concentration of protein in pore, kg·m^{-3}
C_0 = concentration of protein in bulk solution, kg·m^{-3}
C_e = concentration of protein in eluate, kg·m^{-3}
C_I = initial concentration of protein, kg·m^{-3}
C^* = equilibrium concentration of protein in liquid phase, kg·m^{-3}
ΔC = concentration difference of adsorbate in pore between both sides of diaphragm cell, kg·m^{-3}
d = density of solution, kg·m^{-3}
d_p = particle diameter, m
D_{eff} = intraparticle effective diffusivity, m^2·s^{-1}
D_L = liquid phase diffusivity, m^2·s^{-1}
D_P = pore diffusivity based on parallel diffusion model, m^2·s^{-1}
D_P' = pore diffusivity based on pore diffusion control, m^2·s^{-1}
D_{Pa} = approximate pore diffusivity determined from the slope of the plots according to Eq. 28, m^2·s^{-1}
D_S = surface diffusivity based on parallel diffusion model, m^2·s^{-1}
F = fractional attainment of equilibrium
K = Langmuir equilibrium constant, m^3·kg^{-1}
K^* = slope of equilibrium isotherm (moles adsorbed m^{-3} of solid)/(moles of adsorbate m^{-3} of gas)
q = concentration of protein adsorbed on pore wall, kg·m^{-3} wet adsorbent
q^* = equilibrium concentration of protein in resin-phase, kg·m^{-3} wet adsorbent
$\bar{q}$ = mean concentration of protein adsorbed on pore wall, kg·m^{-3} wet adsorbent
q_0 = adsorbent phase concentration of protein in equilibrium with C_0, kg·m^{-3} wet adsorbent
q_∞ = saturation capacity, kg·m^{-3} wet adsorbent
Δq = adsorbent phase concentration difference between both sides of diaphragm cell, kg·m^{-3} wet adsorbent
$\underline{Q}$ = $q+\epsilon C$, kg·m^{-3} wet adsorbent
$\bar{Q}$ = $\bar{q}+\epsilon C$, mean concentration of protein in a particle, kg·m^{-3} wet adsorbent
r = radial dimension of adsorbent particle, m
r_0 = radius of adsorbent particle, m
R = $1/(1+KC_0)$, dimensionless Langmuir equilibrium constant
Re = $d_p u_f d/\mu$
t = time, s
T = temperature, K
u_f = superficial velocity, m·s^{-1}
V = volume of solution, m^3
V_e = volume of eluate, m^3
W = volume of adsorbent particles, m^3
X = C/C_0
Y = q/q_0

Greek letters

α = $q_0/\epsilon C_0$
β = $\alpha D_S/D_P$
ϵ = porosity of adsorbent
μ = viscosity, kg·m^{-1}·s^{-1}
ρ = r/r_0
τ_P = $D_P t/r_0^2$
τ_S = $D_S t/r_0^2$

Literature Cited

Arnold, F. H., H. W. Blanch, and C. R. Wilke, "Analysis of Affinity Separations: I. Predicting the Performance of Affinity Adsorbers," *Chem. Eng. J.*, **30**, B9 (1985).

Arnold, F. H., H. W. Blanch, and C. R. Wilke, "Analysis of Affinity Separations: II. The Characterization of Affinity Columns by Pulse Techniques," *Chem. Eng. J.*, **30**, B25 (1985).

Arve, B. H., and A. I. Liapis, "Modeling and Analysis of Elution of Biospecific Adsorption in a Finite Bath," *AIChE J.*, **33**, 179 (1987).

Arve, B. H., and A. I. Liapis, "Modeling and Analysis of Elution Stage of Biospecific Adsorption in Finite Bath," *Biotechnol. Bioeng.*, **31**, 240 (1988).

Carslaw, H. S., and J. C. Jaeger, *Conduction of Heat in Solids*, Oxford Univ. Press, London (1959).

Costa, E., G. Calleja, and F. Domingo, "Adsorption of Gaseous Hydrocarbons on Activated Carbon: Characteristic Kinetic Curve," *AIChE J.*, **31**, 982 (1985).

Crank, J., *The Mathematics of Diffusion*, Clarendon Press, Oxford, 2nd ed., 91 (1975).

Evanson, M. A., and H. F. Deutsch, "Influence of Fatty Acids on the Isoelectric Point Properties of Human Serum Albumin," *Clin. Chim. Acta.*, **89**, 341 (1978).
Graham, E. E., and C. F. Fook, "Rate of Protein Absorption and Desorption on Cellulose Ion Exchangers," *AIChE J.*, **28**, 245 (1982).
Hossain, M. M., and D. D. Do, "The Effects of Denaturation in the Displacement Chromatographic Behavior of Proteins," *Chem. Eng. J.*, **49**, B29 (1992).
"Ion Exchange Chromatograph: Principles and Methods," Pharmacia LKB Biotechnology (1990).
James, E. A., and D. D. Do, "Equilibrium of Biomolecules on Ion-Exchange Adsorbents," *J. Chromatog.*, **542**, 19 (1991).
Kawamura, Y., M. Mitsuhashi, H. Tanibe, and H. Yoshida, "Adsorption of Metal Ions on Polyaminated Highly Porous Chitosan Chelating Resin," *Ind. Eng. Chem. Res.*, **32**, 386 (1993).
Levenspiel, O., *Chemical Reaction Engineering*, Wiley, New York, p. 346 (1966).
Liapis, A. I., "Modeling Affinity Chromatography," *Sep. and Purif. Methods*, **19**, 133 (1990).
McCoy, M. A., and A. I. Liapis, "Evaluation of Kinetic Models for Biospecific Adsorption and Its Implications for Finite Bath and Column Performance," *J. Chromatog.*, **548**, 25 (1991).
Suzuki, M., *Adsorption Engineering*, Kodansha/Elsevier, Tokyo and Amsterdam, p. 65 (1990).
Takeuchi, Y., E. Furuya, and H. Ikeda, "On the Concentration Dependency of Intraparticle Effective Diffusivity for Tetrahydrofuran-Activated Carbon System," *J. Chem. Eng. Jpn.*, **17**, 304 (1984).
Tilton, R. D., C. R. Robertson, and A. P. Gast, "Lateral Diffusion of Bovine Serum Albumin Adsorbed at the Solid-Liquid Interface," *J. Colloid and Interface Sci.*, **137**, 192 (1990).
Tsou, H. S., and E. E. Graham, "Prediction of Adsorption and Desorption of Protein on Dextran Based Ion-Exchange Resin," *AIChE J.*, **31**, 1959 (1985).
Tyn, M. T., and T. W. Gusek, "Prediction of Diffusion Coefficients of Proteins," *Biotechnol. Bioeng.*, **35**, 327 (1990).
Wallevik, K., "Isoelectric Focusing of Bovin Serum Albumin Influence of Binding of Carrier Ampholites," *Biochim. Biophys. Acta*, **322**, 75 (1973).
Weisz, P. B., and R. D. Goodwin, "Combustion of Carbonaceous Deposits within Porous Catalyst Particles: I. Diffusion Controlled Kinetics," *J. Cat.*, **2**, 397 (1963).
Wen, C. Y., "Noncatalytic Heterogeneous Solid-Fluid Reaction Models," *Ind. Eng. Chem.*, **60**, 34 (1968).
Yagi, S., and D. Kunii, "Theory on Roasting of Sulfide Ore with Uniform Particle Diameter in Fluidized Bed," *Kogyou-Kagaku-Zassi*, **56**, 131 (1953).
Yamamoto, S., K. Nakanishi, R. Matsuno, and T. Kamikubo, "Ion Exchange Chromatography of Protein—Prediction of Elution Curves and Operation Conditions: II. Experimental Verification," *Biotechnol. Bioeng.*, **25**, 1373 (1983).
Yoshida, H., H. Nishihara, and T. Kataoka, "Adsorption of BSA on Strongly Basic Chitosan: Equilibria," *Biotechnol. Bioeng.*, **43**, 1087 (1994).
Yoshida, H., H. Nishihara, and T. Kataoka, "Adsorption of BSA on QAE-Dextran: Equilibria," *Biotechnol. Bioeng.*, **41**, 280 (1993).
Yoshida, H., M. Maekawa, and M. Nango, "Parallel Transport by Surface and Pore Diffusion in a Porous Membrane," *Chem. Eng. Sci.*, **46**, 429 (1991).
Yoshida, H., and T. Kataoka, "Adsorption of BSA on Cross-linked Chitosan: The Equilibrium Isotherm," *Chem. Eng. J.*, **41**, B11 (1989).
Yoshida, H., and T. Kataoka, "Intraparticle Ion-Exchange Mass Transfer in Ternary System," *Ind. Eng. Chem. Res.*, **26**, 1179 (1987).

Manuscript received July 26, 1993, and revision received Nov. 30, 1993.